

# A simple non-quasi-static non-linear model of electron devices

A. Santarelli<sup>1</sup>, V. Di Giacomo<sup>1</sup>, A. Raffo<sup>2,3</sup>,  
P. A. Traverso<sup>1</sup>, G. Vannini<sup>2</sup>, F. Filicori<sup>1</sup>, V. A. Monaco<sup>1</sup>

<sup>1</sup>University of Bologna, Department of Electronics, Viale Risorgimento, 2, 40136 Bologna, Italy,  
e-mail: asantarelli@deis.unibo.it

<sup>2</sup>University of Ferrara, Department of Engineering, Via Saragat, 1, 44100 Ferrara, Italy

<sup>3</sup>CoRiTel, Via Anagnina 203, 00040 Morena (Roma), Italy

**Abstract** — A technology-independent, non-quasi-static non-linear model of electron devices capable of accurate predictions at microwave and millimetre waves is proposed in this paper. The model is based on the definition of a quasi-static associated device, which is controlled by means of equivalent voltages. In particular, in the paper it is shown how to define and experimentally identify suitable voltage-controlled voltage sources, which modify the original domain of applied voltages and create a suitable control environment for the purely-quasi-static associated device. The advantage of this approach is that conventional purely quasi-static models can still be adopted even at very high frequencies, if suitable equivalent voltages are applied. Preliminary experimental validation of the approach is provided in the paper by means of a GaAs PHEMT.

## I. INTRODUCTION

Quasi-static intrinsic device model approaches [1] are often based on well-known lumped equivalent circuit topologies. However, the frequency validity range of these models is very limited due to non-quasi-static phenomena, if suitable corrections are not adopted. To this aim, common non-quasi-static approaches, such as [2]-[4], are based on modified current sources and/or on "delayed" charges and/or on the introduction of series resistors as in Fig.1. These models are in general sufficiently accurate up to very high frequencies. However, their identification and implementation can be not so easy since non-quasi-static phenomena are described by equations and/or circuit elements, which are non-linear. In the proposed approach, instead, non-quasi-static effects are described by linear, frequency-dependent voltage generators, which are applied to an associated quasi-static non-linear model and that can be easily identified from conventional measurements and directly implemented in the framework of CAD-oriented tools.

## II. THE NON-QUASI-STATIC MODEL

We consider a strictly-intrinsic device, i.e. the device obtained after de-embedding from extrinsic parasitic elements and from the components<sup>1</sup> of a purely-capacitive

<sup>1</sup> These are only weakly non-linear dependent on the intrinsic voltages and can be possibly approximated by linear capacitors.

parallel network, which describe the behaviour of the intrinsic device in the off-state (i.e.  $v_{GS} < V_T$ ). In such a way, the strictly-intrinsic transistor has the property of becoming an open circuit in the pinched-off region. The behaviour of the device at the strictly-intrinsic ports may be described by the well-known charge-controlled vector equations:

$$\begin{cases} i(t) = \Phi\{q(t)\} + \frac{dq(t)}{dt} \\ q(t) = \Psi\{v(t)\} \end{cases} \quad (1)$$

Unfortunately, non-quasi-stationary phenomena occur in the device at increasingly high frequencies, which are not taken into account in (1). In particular, charge carriers need finite times for re-arranging the channel status after fast gate-source and gate-drain voltage variations. These phenomena could be described by substituting the second equation in (1) by means of:

$$q^{NQS}(t) = \Psi^{NQS}\left[v(t-\tau)\right]_{\tau=0}^{\infty} \doteq q(t) + \Delta q(t), \quad (2)$$

where the instantaneous non-quasi-static charge  $q^{NQS}$  is described by a functional  $\Psi^{NQS}$ , which takes into account non-linear dynamic effects. In (2),  $q^{NQS}(t)$  is not only dependent on the instantaneous voltage  $v(t)$ , but also on the voltages  $v(t-\tau)$  at previous time instants, with  $\tau$  ranging from 0 to  $\infty$  or, without loss of accuracy, to a finite memory time  $T_M$ . Moreover, the non-quasi-static charge may be seen as the summation of the quasi-static charge and a charge perturbation  $\Delta q(t)$ , which is also implicitly defined by (2).

Alternatively, an equivalent result may be obtained by defining an associated non-linear quasi-static device, still described by (1) but controlled by equivalent voltages  $v^{QS}(t)$ , defined by:

$$\begin{aligned} v^{QS}(t) &= \Psi^{-1}\{q^{NQS}(t)\} = \Psi^{-1}\{\Psi\{v(t)\} + \Delta q(t)\} \\ &\doteq v(t) + \Delta v(t). \end{aligned} \quad (3)$$

In particular, the equivalent voltage domain can be obtained, as shown in Fig.2, by means of voltage-controlled voltage sources  $\Delta v(t)$ , which take into account the dynamics of the non-quasi-stationary phenomena occurring in the device. We adopt for the  $\Delta v(t)$  terms the following model:

$$\Delta v(t) = \int_0^{\infty} a(\tau) \cdot [v(t-\tau) - v(t)] d\tau, \quad (4)$$

where, for simplicity sake, linearity has been assumed with respect to the voltage. The dependence on the dynamic voltage deviation  $v(t-\tau)-v(t)$  in the convolution integral allows for a vanishing contribution of (4) when the signal frequencies involved are not large enough to generate a non-quasi-static behaviour. Simple Fourier-transforming of (4) leads to the frequency-domain expression of the linear voltage-controlled voltage sources:

$$\Delta V(\omega) = A(\omega) \cdot V(\omega). \quad (5)$$

By inspection of Fig.2, we have:

$$I = Y \cdot V = Y^{QS} \cdot V^{QS} = Y^{QS} \cdot (V + \Delta V), \quad (6)$$

where  $Y$  and  $Y^{QS}$  are the admittance matrix of the strictly-intrinsic device and of the associated quasi static device, respectively. The  $Y$  matrix can be directly obtained at different biases and frequencies by means of measurements after de-embedding of parasitic and parallel off-state capacitive elements. Moreover, the voltage sources defined in (5) give a negligible contribution in a frequency range where reactive effects are rather important but non-quasi-stationary phenomena are still negligible. Thus, the  $Y^{QS}$  matrix, describing the bias- and frequency-dependent small-signal behaviour of the associated quasi-static device may be simply identified on the basis of the complex admittance parameters of the strictly-intrinsic device in this frequency range.

Substituting (5) in (6), after simple algebraic manipulation, we have:

$$(Y^{QS})^{-1} \cdot Y = 1 + A, \quad (7)$$

which can be used for the identification of the dynamic-voltage sources (5), i.e. of the  $A$  matrix at each frequency. More precisely, a multi-bias best fit procedure based on (7) may be used for the identification of the  $A$  matrix elements on a suitable frequency range extending to the region where non-quasi-stationary phenomena occur.

Alternatively, the integral in (4) can be practically truncated to the finite memory time  $T_M$  and approximated by a discrete convolution, where the memory time  $T_M$  is divided into  $N_D$  elementary time slots  $\Delta\tau$  (i.e.  $T_M = N_D \Delta\tau$ ):

$$\Delta v(t) \cong \sum_{p=1}^{N_D} a_p \cdot [v(t - p\Delta\tau) - v(t)], \quad (8)$$

where  $a_p$  are suitable scalar parameters to be identified. A number of three intervals has been chosen in our work.

By considering (8) in the frequency domain, we obtain the alternative expression of the linear, frequency-dependent voltage-controlled voltage sources:

$$\Delta V(\omega) \cong \left( \sum_{p=1}^{N_D} a_p (e^{-j\omega p\Delta\tau} - 1) \right) \cdot V(\omega). \quad (9)$$

Substituting (9) in (6) yields now:

$$(Y^{QS})^{-1} \cdot Y \cong 1 + \sum_{p=1}^{N_D} a_p (e^{-j\omega p\Delta\tau} - 1). \quad (10)$$

Thus, identification of the linear voltage controlled voltage sources, i.e. of the  $a_p$  model parameters in this case, may be based on (10), instead of (7).

### III. CAD IMPLEMENTATION

The non-quasi-static device model was implemented in the Agilent ADS CAD environment. To this aim, a previously proposed PHEMT model [5] describing the low-frequency<sup>2</sup> behaviour of the device was adopted (the model also takes into account the low-frequency dispersive effects due to self-heating and charge trapping phenomena). Moreover, the quasi-static reactive effects of the strictly-intrinsic device were modelled by means of a Symbolically Defined Device using look-up-table based bias-dependent quasi-static capacitors. Then, the voltage-controlled voltage sources were implemented in series at the gate electrode only, as shown in Fig.3. This choice led in our experiments to sufficiently accurate results, without the need for introducing corresponding voltage sources at the drain electrode.

In this case, by adopting the non-truncated memory expression (5), the model becomes fully identified when the  $A_{11}(\omega)$  and  $A_{12}(\omega)$  functions are known. Alternatively, by choosing (9) the model parameters reduce to only six scalar quantities. The difference between the two kind of identifications may be, for instance, seen in Fig.4.

### IV. EXPERIMENTAL VALIDATION

The proposed model was identified for a GaAs PHEMT ( $L = 0.25 \mu\text{m}$ ,  $W = 600 \mu\text{m}$ ). To this aim, a memory time  $T_M = 1,8\text{ps}$  with  $N_D = 3$  was chosen. A multi-bias and multi-frequency dc and ac small-signal characterization of the DUT was carried out up to 70 GHz. After identification of extrinsic parasitic elements by means of known cold FET procedures, a linear parallel network of purely-quasi-static capacitors was identified at pinched-off channel conditions, leading to:  $C_{GS} = 172\text{fF}$ ,  $C_{GD} = 103\text{fF}$ ,  $C_{DS} = 123\text{fF}$ . After de-embedding from these elements, the bias-dependent quasi-static capacitance matrix of the strictly-intrinsic device was identified on the basis of the imaginary part of admittance parameters in a frequency range between 1 and 10 GHz, where the device behaviour was found to be nearly quasi-static. The capacitor values were then stored into CAD-based look-up-tables. Finally, a multi-bias identification of the six  $a_p$  model parameters led to the full determination of the model.

Model validation was carried out by comparing predictions of small-signal parameters up to 70 GHz with measurements at the intrinsic device ports. Typical results

<sup>2</sup> The model described in [5] is capable of accurate predictions in the presence of signal frequencies, which are above the cut-off of dispersive phenomena but low enough to allow for neglecting the transistor reactive effects.

are shown in Fig.5, where the "virtual" quasi-stationary behaviour is also shown as a reference. As can be seen, important corrections by the model voltage-sources are needed for accurate predictions. Moreover, although the adopted voltage-sources are linear and bias-independent, analogous results were obtained at very different bias conditions, as shown, for instance, in Fig. 6. Bias-dependent intrinsic admittances at the frequency of 40GHz are compared with measured data in Fig.7. Finally, the model was experimentally validated under non-linear device operation. Model intermodulation distortion predictions at 37 GHz are compared in Fig.8 with measurements, showing great accuracy even at the extremely low levels of the third-order intermodulation products.

### V. CONCLUSIONS AND FUTURE WORKS

A new technology-independent, non-quasi-static non-linear model of electron devices has been presented. The model is easy to extract and implement in CAD environments, and it provides good predictions both in small- and large-signal analyses. Possible model improvements will be investigated by considering the  $\Phi$  function in the current equation (1) not only dependent on the charge  $q(t)$  but also on the applied voltage  $v(t)$ .

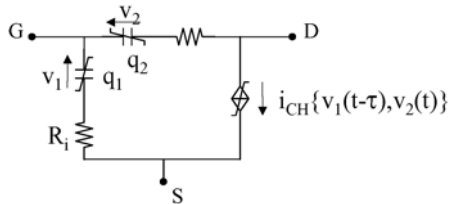


Fig. 1 - Typical corrections to take into account non-quasi-stationary phenomena in classical models.

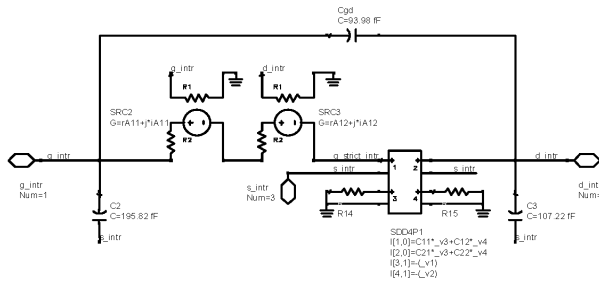


Fig. 3 - CAD implementation of the non-quasi-static model in the Agilent ADS CAD tool.

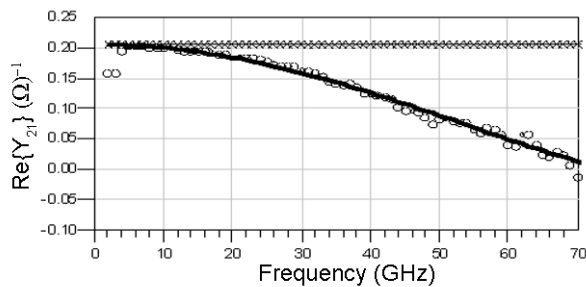


Fig. 5 - Prediction of the intrinsic PHEMT admittance parameters by means of the proposed modelling approach. Bias:  $I_D = 60$  mA,  $V_{DS} = 6.5$  V. Legend:  $\circ$  = measurement, — = proposed model, x = purely stationary model.

### ACKNOWLEDGEMENT

This work was partly funded by MIUR (Italian Ministry of Instruction, University and Research) and also performed in the context of the Network of Excellence TARGET – “Top Amplifier Research Groups in a European Team” supported by the Information Society Technologies Programme of the EU under contract IST-1-507893-NOE, www.target-net.org.

### REFERENCES

- [1] M. J. Golio, *Microwave MESFETs and HEMTs*, Artech House, 1991.
- [2] W. R. Curtice, “A MESFET model for use in the design of GaAs integrated circuits”, *IEEE TMTT*, vol. 28, May 1980.
- [3] R. R. Daniels et al. “A universal large/small signal 3-terminal FET model using a nonquasi-static charge-based approach”, *IEEE Trans. Electron Devices*, vol.40, Oct. 1993.
- [4] M. Fernández-Barciela et al., “A simplified broadband large signal non quasistatic table-based FET model”, *IEEE TMTT*, vol. 48, Mar. 2000.
- [5] F.Filicori et al., “Empirical modeling of low-frequency dispersive effects due to traps and thermal phenomena in III-V FET’s,” *IEEE Trans. Microwave Theory and Techn.*, vol. 43, Dec. 1995.

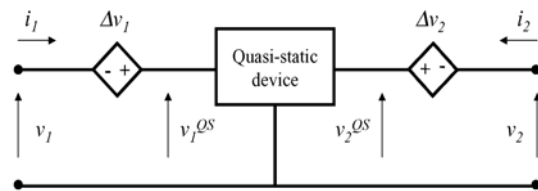


Fig. 2 - Circuit schematic of the proposed non-quasi-static modelling approach for the strictly-intrinsic device.

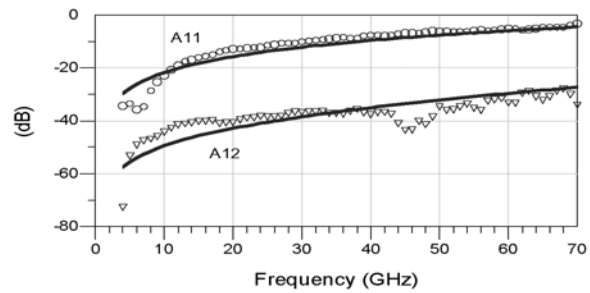
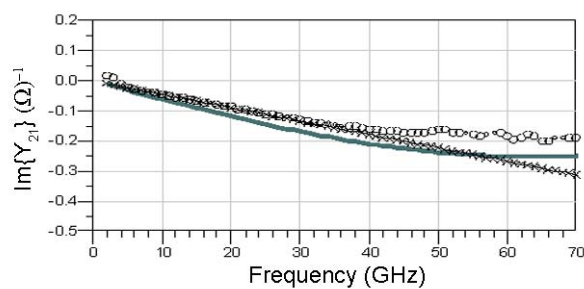


Fig. 4 - Gains of controlled voltage sources obtained with (line) and without (symbols) memory truncation.



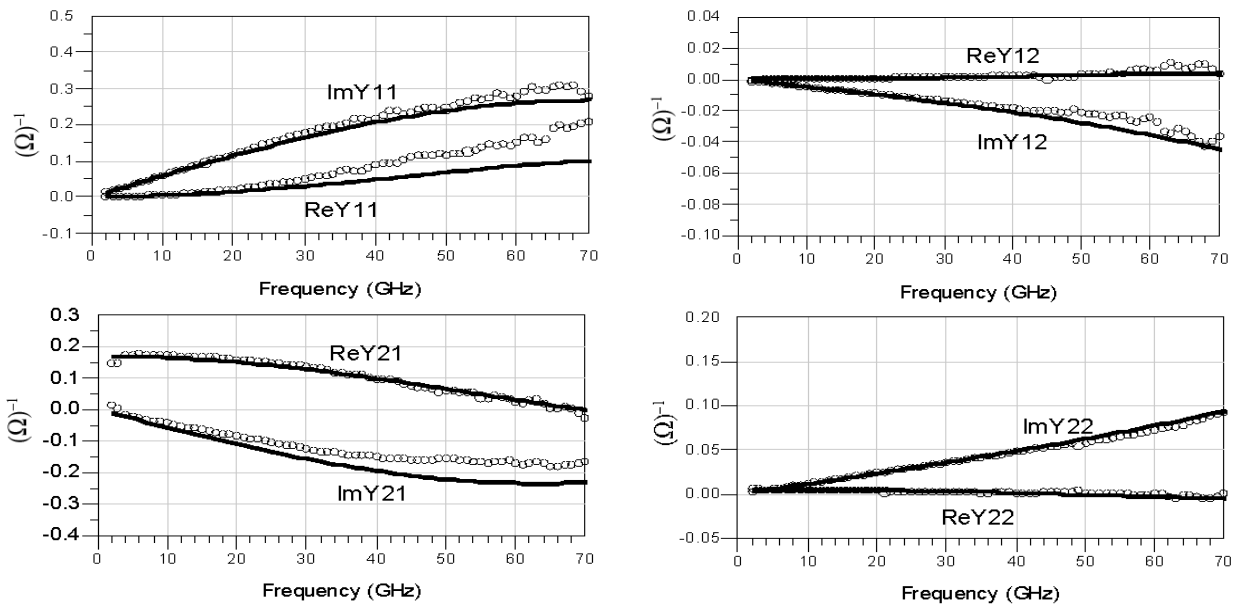


Fig. 6 – Intrinsic PHEMT admittance parameters predicted by the non-quasi-static model. Bias:  $I_D=30\text{mA}$ ,  $V_{DS}=7.5\text{V}$ . Legend:  $\circ$  = measurements, — = proposed model.

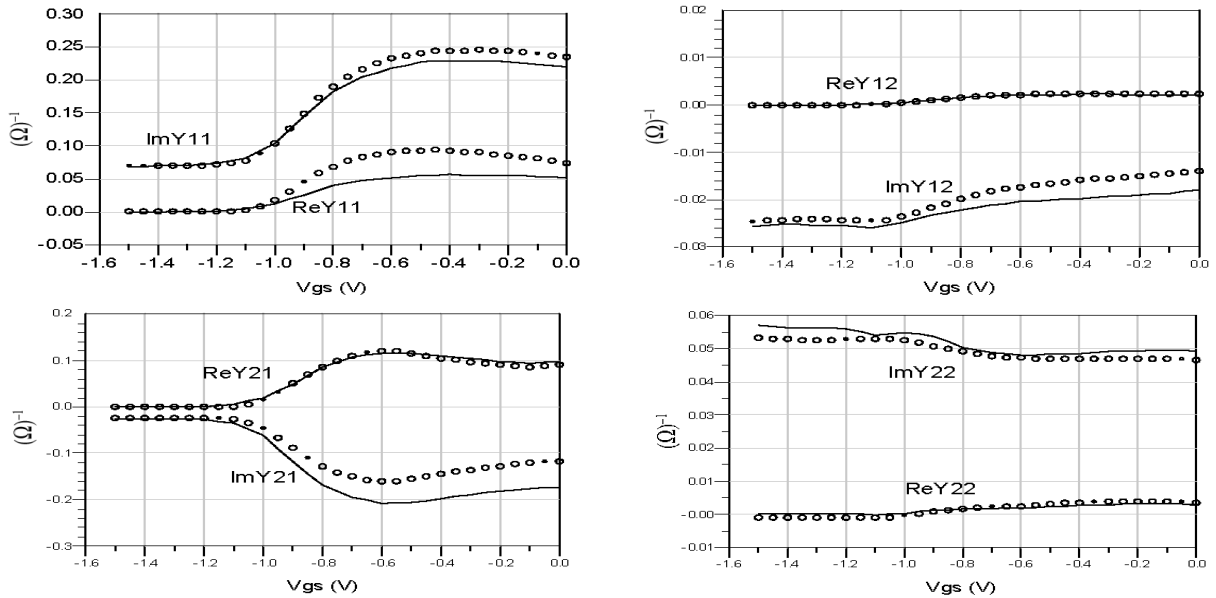


Fig. 7 - Prediction of PHEMT intrinsic admittance parameters at the frequency of 40GHz, where non-quasi-stationary effects are relevant, at  $V_{DS}=6.5\text{V}$ . Legend:  $\circ$  = measurements, — = model. As it is evident, very good performance is also obtained in the pinched-off region, thanks to the choice of identifying the model at the *strictly-intrinsic* device sections (see text).

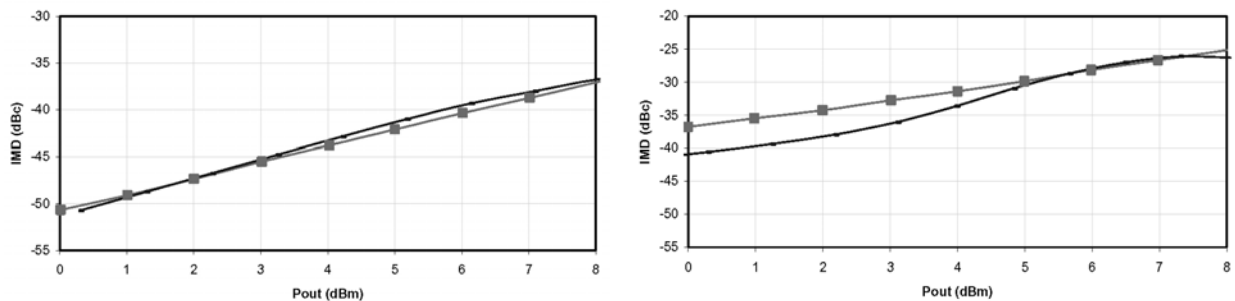


Fig. 8 – PHEMT third-order intermodulation distortion at  $f_0=37\text{GHz}$ .  $\Gamma_L = 0.56\angle 156^\circ$ ,  $\Gamma_S = 0.09\angle -87^\circ$ ,  $I_D=60\text{mA}$ ;  $V_{DS}=6.5\text{V}$  (left);  $\Gamma_L = 0.24\angle -177^\circ$ ,  $\Gamma_S = 0.08\angle -130^\circ$ ,  $I_D=15\text{mA}$ ;  $V_{DS}=5.5\text{V}$  (right). Legend: square = measurement, continuous line = proposed approach.